16th World Conference on Earthquake, 16WCEE 2017
Santiago Chile, January 9th to 13th 2017
Paper N° 733 (Abstract ID)
Registration Code: S-S1462868735

MINIMUM-COST OPTIMAL DESIGN OF NONLINEAR FLUID VISCOUS DAMPERS AND THEIR SUPPORTING BRACES FOR SEISMIC RETROFITTING

N. Pollini[(1)], O. Lavan[(2)], O. Amir[(3)]

[(1)] PhD Student, Faculty of Civil and Environmental Engineering, Technion – Israel Institute of Technology, nicolo@campus.technion.ac.il
[(2)] Associate Professor, Faculty of Civil and Environmental Engineering, Technion – Israel Institute of Technology, lavan@cv.technion.ac.il
[(3)] Assistant Professor, Faculty of Civil and Environmental Engineering, Technion – Israel Institute of Technology, odedamir@cv.technion.ac.il

Abstract

In this paper, we present a new methodology for achieving economical retrofitting design solutions of 3-D irregular frames. Nonlinear fluid viscous dampers and their supporting braces are optimally distributed in irregular 3D frames and optimally sized. For generating optimal design solutions useful for practitioners, a realistic cost formulation is chosen as the objective function to be minimized. Constraints are imposed on inter-story drifts at the peripheries. These are evaluated with nonlinear time-history analyses considering realistic ground acceleration records. The behavior of each damper-brace system is defined based on the Maxwell's model for viscoelasticity. A fractional power-law is used to describe the nonlinear force-velocity relation of each damper, and the stiffening contribution of the supporting brace and of the damper is represented by linear springs. The damper-brace elements are divided into size-groups, that is, elements with the same mechanical properties. The properties of each size-group of dampers (damping coefficient and supporting brace stiffness), and the dampers' distribution in the structure are optimally defined in the optimization process using Genetic Algorithms. The capability of the proposed methodology to achieve economical designs is demonstrated in a practical case. The numerical results establish also important benchmarks for other, more efficient, methods to be developed.
Keywords: nonlinear fluid viscous dampers; Maxwell's model; irregular frames; nonlinear time history analysis; genetic algorithm.

1. Introduction

Earthquakes keep on being a major source of threat for those communities located in seismic areas. Too often this threat results in human losses and disruption of commercial activities. It is in this context that in recent years performance-based design became very popular among engineers ([1], [2]). It allows, in fact, to design buildings able to withstand different levels of seismic hazard with desired levels of performance, hence safety. This is also true in the case of existing buildings, where one of the most advantageous seismic retrofitting techniques is the use of passive devices. In many cases, in fact, they can prevent the need for columns and foundations strengthening.

Fluid viscous dampers are a very popular type of seismic protection device. They have been successfully used in several branches of the U.S. military, and with the end of the Cold War in 1990 they have been declassified becoming available for civil purposes ([3]). In seismic retrofitting, in particular, they proved to be very effective in reducing both inter-story drifts and total accelerations, [4]. However, it has been shown that the distribution of viscous dampers in the structure can significantly affect their efficiency, [5]. This motivated many researchers in developing optimization-based design approaches for seismic retrofitting with viscous dampers.

The relevant literature can be divided into methodologies for the optimal distribution of dampers with given properties ([6], [7], [8]); methodologies for the optimal distribution of dampers selecting their size from a given set of available dimensions ([9], [4]); methodologies for the optimal distribution of dampers where each damper is represented by an independent continuous variable ([10], [11]); methodologies for the optimal distribution and sizing of dampers where final discrete solutions are achieved either with a mixed-integer problem formulation ([12], [13]) or with a continuous one ([14], [15]). Even though dampers are typically supported by braces, in the above mentioned methodologies the braces are considered as infinitely stiff. However, if the brace has a finite stiffness the behavior and the performance of the damper-brace system can differ significantly. In practice the braces have an upper limit in terms of their cross section, and the assumption of "infinitely stiff" brace is not always acceptable. Having a limit on the brace dimensions affects also the maximum acceptable damping coefficient: an unproportioned damping coefficient may cause the concentration of stresses and deformation in the brace leading to undesired damper-brace behaviors. This is also supported by recent studies where the brace cross section has been included as a design variable of the problem ([16], [17], [18], [19], [10]).

This paper is presumably the first to address the optimal distribution and sizing of nonlinear fluid viscous dampers together with their supporting braces. Their sizes are chosen from a limited number of size-groups, whose mechanical properties are also variables of the problem. A realistic retrofitting cost function is minimized while constraints are imposed on inter-story drifts at the peripheries of irregular 3-D structures. The structural responses of interest are evaluated with nonlinear time-history analyses, considering realistic ground motion accelerations. We thus provide engineers with a practical tool for the performance-based seismic retrofitting with fluid viscous dampers. Using the proposed method, practitioners can identify minimum-cost designs based on specific cost parameters according to the setting of the retrofitting project.

2. Governing Equations

In the following section we first present the model considered for the definition of the damper-brace behavior and the relative equations. Then, we recall the equations of motion for a structure equipped with nonlinear fluid viscous dampers, and subject to a realistic ground motion acceleration. The formulation presented in this paper it is not limited to a specific structural behavior. However, in the following we will consider a linear structural behavior.

2.1 Damper-brace system characterization

In this work we consider damper-brace systems made of two springs and a dashpot in series, as shown in Fig. 1, ([20]).

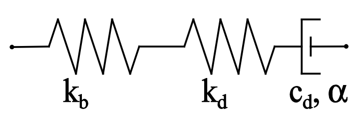

Fig. 1 – Stiffening and damping contributes of the damper-brace system

The first spring accounts for the stiffness of the supporting brace, while the second for the stiffness of the damper. Last, the dashpot accounts for the damping property of each damper. The two springs are modeled with a linear force-displacement behavior, while the dashpot force-velocity behavior is defined by a fractional power law:

$$
\begin{aligned}
f_b &= k_b u_b \\
f_d &= k_d u_d \\
f_d &= c_d \,\mathrm{sign}(\dot{u}_d)|\dot{u}_d|^{\alpha}
\end{aligned}
\qquad (1)
$$

where f_b is the force in the brace, and f_d is the force in the damper; k_b is the brace stiffness, k_d the damper stiffness, and c_d its damping coefficient; u_b is the elongation of the brace, u_d the elongation of the damper, and $\dot{u}_d$ the relative velocity between the ends of the damper. The exponent $0 < \alpha \leq 1$ characterizes the nonlinear behavior of the dashpot. For α equal to one the damper is linear, while for α that tends to zero the formulation mimics the behavior of a friction damper. The exponent α significantly affects the computational effort required for integrating the equations of motion. The algorithm for the time-history analysis developed by the authors and used in this work successfully solved the equations of motion for values of α between 0.1 and 1. Herein we will consider α equal to 0.35, as in [21]. Because of equilibrium, the forces in the damper and in the brace are equal ($f_b = f_d$). It follows that:

$$k_b u_b = k_d u_d = c_d \, \mathrm{sign}(\dot{u}_d) |\dot{u}_d|^{\alpha} \tag{2}$$

The axial stiffness of a brace can be easily calculated. The stiffness contribute of a fluid viscous damper, on the contrary, is far less intuitive. It depends in fact on:

1. The stiffness of the metal parts of the damper from one end to the other;
2. The stiffness of the fluid column inside the damper;
3. The expansion of the damper cylinder under pressure (which makes the fluid seem more compressible).

Among the three components mentioned above, the second is the more complex to be defined. The fluid under pressure behaves according to its bulk modulus curve, which is nonlinear. However, dampers of a single manufacturer typically have their peak forces at similar limit pressures, and in general they are also made of the same materials. Thanks to this, many of the variables drop out. As a result, the end to end stiffness of a fluid viscous damper, as tested by Taylor Devices ([22]), is such that it will reach its rated force at approximately 3% of its rated stroke from the centered position. This defines the stiffness of the damper that can be considered as a constant property of the device.

The ratio between the damping coefficient of a damper and the stiffness of the damper and the brace is very important in the solution of the equations of motion. In fact, it affects the computational effort and the complexity of the integration technique required in each time step. This is particularly true in the case of nonlinear fluid viscous dampers. For this reason, we define a priori the ratio between the damping coefficient of the damper and the equivalent stiffness resulting from the brace and the damper. To pre-assign a reasonable value for this ratio, we consider the structure subject to the Maximum Considered Earthquake. We can thus calculate the maximum inter-story drift (d_{max}) experienced by a given structure. We then subject the damper-brace system to a harmonic displacement history, with amplitude d_{max}, and as frequency the first natural frequency of the structure above 4Hz. It is known, in fact, that dampers behave as pure dashpots for exciting frequencies below a cut-off frequency of approximately 4Hz, [23]. At the maximum force, the damper will have a displacement between its ends equal to the 3% of its maximum stroke. For the same force, we assume that the brace will reach its ultimate displacement allowed (u_y). That is, for F_{max} in the damper-brace system we have that:

- In the brace: $k_b = \frac{F_{max}}{u_y} = \frac{F_{max}}{\epsilon_y L_b}$;
- In the damper: $k_d = \frac{F_{max}}{\text{stroke } 0.03}$.

With regards to the brace, for example: $u_y = \epsilon_y L_b = \frac{f_y}{E_s} L_b = \frac{235\text{MPa}}{210\text{GPa}} 6000\text{mm} = 6.7\text{mm}$. For the damper we consider a rated stroke of ±4 inches=±10.16cm. Hence:

$$k_{eq} = \frac{F_{max}}{u_b + u_d} = \frac{F_{max}}{\epsilon_y L_b + 3\%\text{stroke}} = \frac{F_{max}}{6.7\text{mm} + 3.05\text{mm}} \cong \frac{c_d \, \mathrm{sign}\left(\dot{u}^d_{max}\right) |\dot{u}^d_{max}|^{\alpha}}{10\text{mm}} \tag{3}$$

In particular, the ratio ρ is:

$$\rho = \frac{k_{eq}}{c_d} = 0.1 c_d \, \mathrm{sign}\left(\dot{u}^d{}_{max}\right) |\dot{u}^d{}_{max}|^{\alpha} \tag{4}$$

In the last equation both ρ and $\dot{u}^d{}_{max}$ are unknown, since they depend one upon each other. Through an iterative procedure is possible to evaluate both of them, as illustrated in Fig. 2:

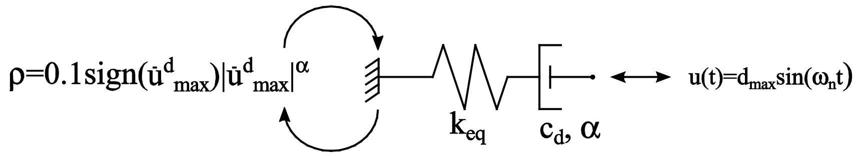

Fig. 2 – Damper-brace tuning procedure

Once the ratio ρ is defined, we can express k_{eq} as:

$$k_{eq}=\rho c_d \tag{5}$$

Therefore, for each damper-brace element the damping coefficient c_d is the design variable, for a given ratio ρ and exponent α (Fig. 3).

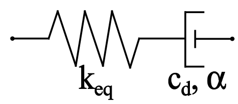

Fig. 3 – Equivalent Maxwell's model for the brace-damper system

2.2 Equations of motion

We consider generic 3-D irregular frames subject to an ensemble of realistic ground motions. Their behavior is characterized by the mass matrix $\mathbf{M}$, the inherent damping matrix $\mathbf{C}_s$, and the stiffness matrix $\mathbf{K}_s$. Nonlinear damper-brace elements are distributed in predefined potential locations of the structure. They all share the same ratio ρ, and exponent α, that have been already presented in Sec. 2.1. Each damper is characterized by a specific damping coefficient c_d.

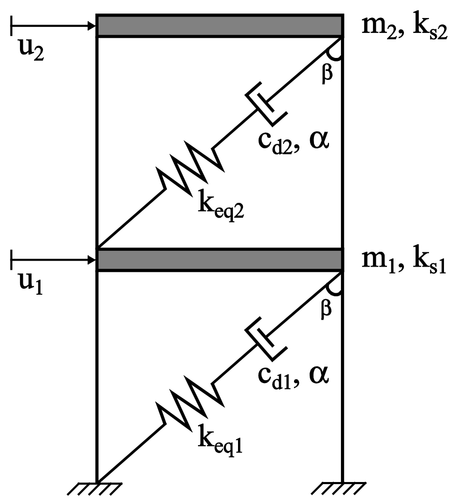

Fig. 4 – Two degrees of freedom system with nonlinear fluid viscous dampers

The responses of interest are evaluated with nonlinear time-history analyses. For each point *t* in time, the dynamic behavior of a structure with N_{dof} degrees of freedom and N_d potential location for dampers is defined by a set of N_{dof} second order differential equations, coupled with a set of N_d first order differential equations as follows:

$$\mathbf{M}\ddot{\mathbf{u}}(t)+\mathbf{C}_s\dot{\mathbf{u}}(t)+\mathbf{K}_s\mathbf{u}(t)+\mathbf{T}^T\mathbf{f}_d(t)\sin(\beta)=-\mathbf{M}\mathbf{e}a_g(t) \tag{6}$$

$$\mathbf{f}_d(t)=D(\mathbf{k}_{eq})\left[\mathbf{T}\dot{\mathbf{u}}(t)\sin(\beta)-\left(D(\mathbf{c}_d)^{-1}D(|\mathbf{f}_d(t)|)\right)^{\frac{1}{\alpha}}\mathrm{sign}(\mathbf{f}_d(t))\right]$$

In Eq. (6) $\mathbf{u}(t)$ is the displacement vector of the degrees of freedom; $\mathbf{f}_d(t)$ the vector of the resisting forces of the dampers; β the angle between the local degrees of freedom of the dampers and the global degrees of freedom; $\mathbf{e}$ is the location vector that defines the location of the excitation; and $a_g(t)$ is the ground acceleration. $D(\cdot)$ is an operator that transforms a vector into a diagonal matrix, and a diagonal matrix into a vector (as the *diag* MATLAB function does). The matrix $\mathbf{T}$ is a transformation matrix, that transforms the global coordinates for the displacements and velocities ($\mathbf{u}$, $\dot{\mathbf{u}}$) into local coordinates ($\mathbf{d}$, $\dot{\mathbf{d}}$), namely inter-story drifts and velocities. In the example of Fig. 4 the global coordinates are u_1 and u_2. The local coordinates are $d_1 = u_1$, and $d_2 = u_2 - u_1$. A similar transformation applies to $\dot{\mathbf{u}}_1$ and $\dot{\mathbf{u}}_2$.

In order to be solved, the problem is first discretized in time, and then solved with the Newmark-β method. In particular, in each time step the equilibrium is achieved by means of an iterative procedure. In this procedure, in each step the dampers' forces are approximated with a fourth-order explicit Runge-Kutta method, as suggested in [20]. For more details on Runge-Kutta methods please refer to [24]. The structural response is then corrected with the Newton-Raphson method. The iterative procedure stops when the residual forces are sufficiently small.

3. Optimization problem formulation

In this paper we formulate and solve the problem for the optimal distribution and sizing of nonlinear fluid viscous dampers. A realistic retrofitting cost function is minimized while selected structural performance indices are limited to maximum allowable values. The dampers are chosen from two available size-groups, and distributed in potential locations of a given structure. The properties of each size-group are also optimized and not predefined. Thus, in this section we present the design variables involved in the problem formulation, the new retrofitting cost function, and the constrained performance indexes.

3.1 Design variables

The goal is to size and distribute up to N_d nonlinear fluid viscous dampers in predefined potential locations of a given frame. They can be chosen out of two available size-groups, where for size-group we intend a group of dampers with the same characteristics. Therefore, we have to determine N_d damping coefficients c_{di}, that are collected in the vector $\mathbf{c}_d$. The vector of damping coefficients is defined as follows:

$$\mathbf{c}_d=\bar{c}_d\mathbf{x}_1\left(y_1+\left(y_2-y_1\right)\mathbf{x}_2\right) \tag{7}$$

In Eq. (7), $\bar{c}_d$ represents the maximum damping coefficient available, and it is defined a priori. The vector $\mathbf{x}_1$ has binary entries representing the existence of a damper in each potential locations. In particular, a value of zero in the *i*-th entry of the vector will mean that in the location *i* there is no damper, while a value of one that there is a damper. Also $\mathbf{x}_2$ is a vector with binary entries, representing the association of each existing damper to one of the two available size-groups. In the case of x_{2i} equal to zero, the damper in the *i*-th location belongs to the first size-group. In the case of x_{2i} equal to one, the damper in the *i*-th location belongs to the second size-group. We should also mention that the dimensions of the vectors $\mathbf{c}_d$, $\mathbf{x}_1$, and $\mathbf{x}_2$ are $N_d \times 1$. The two available damping coefficients that define the two size-groups are:

$$\mathbf{c}_{d1}=\bar{c}_d y_1, \quad \mathbf{c}_{d2}=\bar{c}_d y_2 \tag{8}$$

In Eq. (8), y_1 and y_2 are two continuous design variables that scale the maximum available damping coefficient $\bar{c}_d$. Last, it should be noted that the design indirectly extends also to the dampers' supporting braces through the parameter ρ, as it has already been illustrated in Sec. 2.1.

3.2 Cost function

One of the main contributions of the present work consists in minimizing a realistic retrofitting cost function. The cost function is inspired by the one presented in [13], and it is further enhanced and more realistic. Therefore, also in this case the cost function J consists of three cost components:

$$J=J_l+J_m+J_p \tag{9}$$

The first cost component J_l represents the cost associated with the number of locations in which dampers are installed. We allow the algorithm to allocate as many as one damper in each potential location; hence, this component includes all costs associated with the preparation of the structure for the damper installation and the architectural constraint that this installation will represent. Moreover, in case of retrofitting, it can also account for the removal of existing nonstructural components. The first component of the cost is defined as follows:

$$J_l=\mathbf{C}_l^T\mathbf{x}_1 \tag{10}$$

where $\mathbf{C}_l$ is a $N_d\times1$ vector in which the *i*-th component is a cost component related to the *i*-th component of $\mathbf{x}_1$.

The second cost component, J_m, represents the manufacturing cost of the dampers. In principle, the manufacturing cost of viscous dampers depends on the peak stroke and on the square root of the peak force of the most loaded damper of each size-groups ([11]). We assume, in fact, that all dampers of a specific size-group are designed so to have the same capacity. Since we are constraining inter-story drifts, also the peak stroke of the dampers is indirectly limited. As a consequence, it does not affect significantly the cost. Therefore, the manufacturing cost is defined as the square root of the peak force of the most loaded damper from each size-group, multiplied by the number of dampers of each size-group. Formally, it is written as follows:

$$J_m=C_m\left\{\mathbf{x}_1^T(\mathbf{1}\text{-}\mathbf{x}_2)\left[\max(\hat{\mathbf{f}}_{d1})\right]^{0.5}+\mathbf{x}_1^T\mathbf{x}_2\left[\max(\hat{\mathbf{f}}_{d2})\right]^{0.5}\right\} \tag{11}$$

where C_m is a scalar cost component which gives the desired proportion between J_m and the other cost components, and:

$$\begin{aligned}&\hat{\mathbf{f}}_{d1}=D(\mathbf{1}\text{-}\mathbf{x}_2)\hat{\mathbf{f}}_d\\&\hat{\mathbf{f}}_{d2}=D(\mathbf{x}_2)\hat{\mathbf{f}}_d\\&\hat{\mathbf{f}}_d=\max_t\left(|\mathbf{f}_d(t)|\right)\end{aligned} \tag{12}$$

$\hat{\mathbf{f}}_d$ is the vector of the peak forces in time for all dampers; the vector $\hat{\mathbf{f}}_{d1}$ has the components of $\hat{\mathbf{f}}_d$ which belongs to dampers of the first size-group, while $\hat{\mathbf{f}}_{d2}$ those of the second size-group. It should be noted that the *max* function in Eq. (11) refers to the components of the vectors $\hat{\mathbf{f}}_{d1}$ and $\hat{\mathbf{f}}_{d2}$, and the result is a scalar. On the contrary, in Eq. (12) the *max* function refers to the maximum absolute value in time for each component of the vector $\mathbf{f}_d(t)$, and the result is a vector.

Modern seismic codes require to test one damper prototype for each size-group so to verify its force-velocity behavior. As a results, we consider an additional cost component, J_p. This component is formulated so that the number of different size-groups of dampers used for retrofitting should be minimized:

$$J_p=C_p\left[H\left(\mathbf{x}_1^T\mathbf{x}_2\right)+H(\mathbf{x}_1^T(\mathbf{1}\text{-}\mathbf{x}_2))\right] \tag{13}$$

where C_p is the cost of prototype testing and design. The function H is the Heaviside step function:

$$H(x)=\begin{cases}1 \text{ for } x>0\\0 \text{ for } x=0\end{cases} \tag{14}$$

We observe that:

- If all dampers are of the first size then J_p will be equal to $C_p \times [0+1]$;
- If all dampers are of the second size then J_p will be equal to $C_p \times [1+0]$;
- In case dampers of both size exist then J_p will be equal to $C_p \times [1+1]$.

3.3 Performance index

We are now considering the seismic retrofitting of 3-D irregular frames using nonlinear fluid viscous dampers. As in [15], here too inter-story drifts are used as an appropriate measure of both structural and nonstructural damage levels. Moreover, by limiting the inter-story drifts it is possible to constrain the response of the structure to a linear behavior. This can be done by limiting the inter-story drifts to the value of drift for which yielding occurs.

In particular, the peak inter-story drift normalized by the allowable value is chosen as the local performance index for 2-D irregular frames:

$$d_{ci} = \max_t \left(\left| d_i(t)/d_{all,i} \right| \right) \leq 1 \quad \forall i=1,\ldots,N_{drifts} \tag{15}$$

where $d_i(t)$ is the inter-story drift *i* at time t; $d_{all,i}$ its maximum allowable value. In the case of 3-D frames, $d_i(t)$ refers to the inter-story drifts of peripheral frames.

3.4 Mixed-integer optimization problem

At this point we have presented all the ingredients of our optimization problem. The following is its mixed-integer formulation:

$$\begin{aligned}
&\min_{\mathbf{x}_1,\mathbf{x}_2,y_1,y_2} \; J=J_1+J_m+J_p \\
&\text{s.t.: } d_{c,i} = \max_t\left(\left|d_i(t)/d_{all,i}\right|\right)\leq 1 \;\; \forall i=1,\ldots,N_{drifts} \\
&x_{1,k}=\{0,1\} \text{ for } k=1,\ldots,N_d \\
&x_{2,k}=\{0,1\} \text{ for } k=1,\ldots,N_d \\
&0\leq y_1^L\leq y_1\leq y_1^U\leq y_2^L \\
&y_1^U\leq y_2^L\leq y_2\leq y_2^U\leq 1 \\
&\text{with } \mathbf{M}\ddot{\mathbf{u}}(t)+\mathbf{C}_s\dot{\mathbf{u}}(t)+\mathbf{K}_s\mathbf{u}(t)+\mathbf{T}^T\mathbf{f}_d(t)\sin(\beta)=-\mathbf{M}\mathbf{e}a_g(t) \;\; \forall a_g\in\mathcal{E} \\
&\dot{\mathbf{f}}_d(t) = D(\mathbf{k}_d)\left[\mathrm{T}\dot{\mathbf{u}}(t)\sin(\beta) - \left(D(\mathbf{c}_d)^{-1}D(|\mathbf{f}_d(t)|)\right)^{\frac{1}{\alpha}}\operatorname{sign}\left(\mathbf{f}_d(t)\right)\right] \\
&\mathbf{u}(0)=\mathbf{0},\; \dot{\mathbf{u}}(0)=0,\; \mathbf{f}_d(0)=\mathbf{0}
\end{aligned} \tag{16}$$

where $\boldsymbol{\mathcal{E}}$ is an ensemble of ground motions considered; N_{drifts} is the number of drifts to be constrained; and $y^L{}_1$, $y^U{}_1$, $y^L{}_2$ and $y^U{}_2$ are user-defined bounds. For optimizing the distribution and size of a single damper size-group, only the $\mathbf{x}_1$ and y_1 variables are necessary, thus it can be seen as a particular case of the two-damper size-group optimization. The problem (16) has been solved with a GA. The results will be presented in Sec. 4.

4. Numerical example

We present now a new numerical example. The goal is to show how the novel problem formulation presented in this paper can be effectively solved, achieving final practical solutions useful for practitioners. For the first time, in fact, nonlinear fluid viscous dampers and their supporting member are optimally sized and distributed into irregular framed structures. A new realistic retrofitting cost function is minimized while limiting the inter-story drifts to allowable values.

In particular we consider an example of an asymmetric frame made of reinforced concrete, as introduced in [25]. This test case was also solved in [14] where a discrete distribution of linear fluid viscous dampers was found, and in [13] where a realistic cost function was minimized achieving also in this case a discrete distribution of damping. The column sizes are 0.5m×0.5m in frames 1 and 2; 0.7m×0.7m in frames 3 and 4 (see Fig. 5). The beam sizes are 0.4m×0.6m and the floor mass is uniformly distributed with a weight of 0.75 ton/m^2. Regarding the ground motion acceleration, out of the ensemble LA 10% in 50 years, LA16 has the largest maximal displacement for reasonable values of the period of the structure. Hence LA16 was the ground motion to be considered first, acting in the y direction ([26]). In the present work, we consider 5% of critical damping for the first two modes in order to build the Rayleigh damping matrix of the structure.

The algorithm used for optimization is a built-in Genetic Algorithm in the MATLAB library. The optimization process automatically stops when one of the following conditions is verified: the number of generations reaches the limit value of generations "*Generations*"; the weighted average change in the fitness function value over "*StallGenLimit*" is less than "*TolFun*". For numerical experiments a parallel-processor MATLAB code was executed on Tamnun, a computer cluster hosted and maintained by the Division for Computing and Information System at the Technion – Israel Institute of Technology.

4.1 Eight-story three bay by three bay asymmetric structure

A plan and two sections of the structure to be optimized are given in Fig. 5. 16 potential locations for dampers were assigned at the peripheral frames in the *y* direction. The allowable inter-story drift d_{all} was set to 0.035 m, and the maximum nominal damping coefficient to $\bar{c}_d$=2000 kN(s/mm)$^\alpha$.

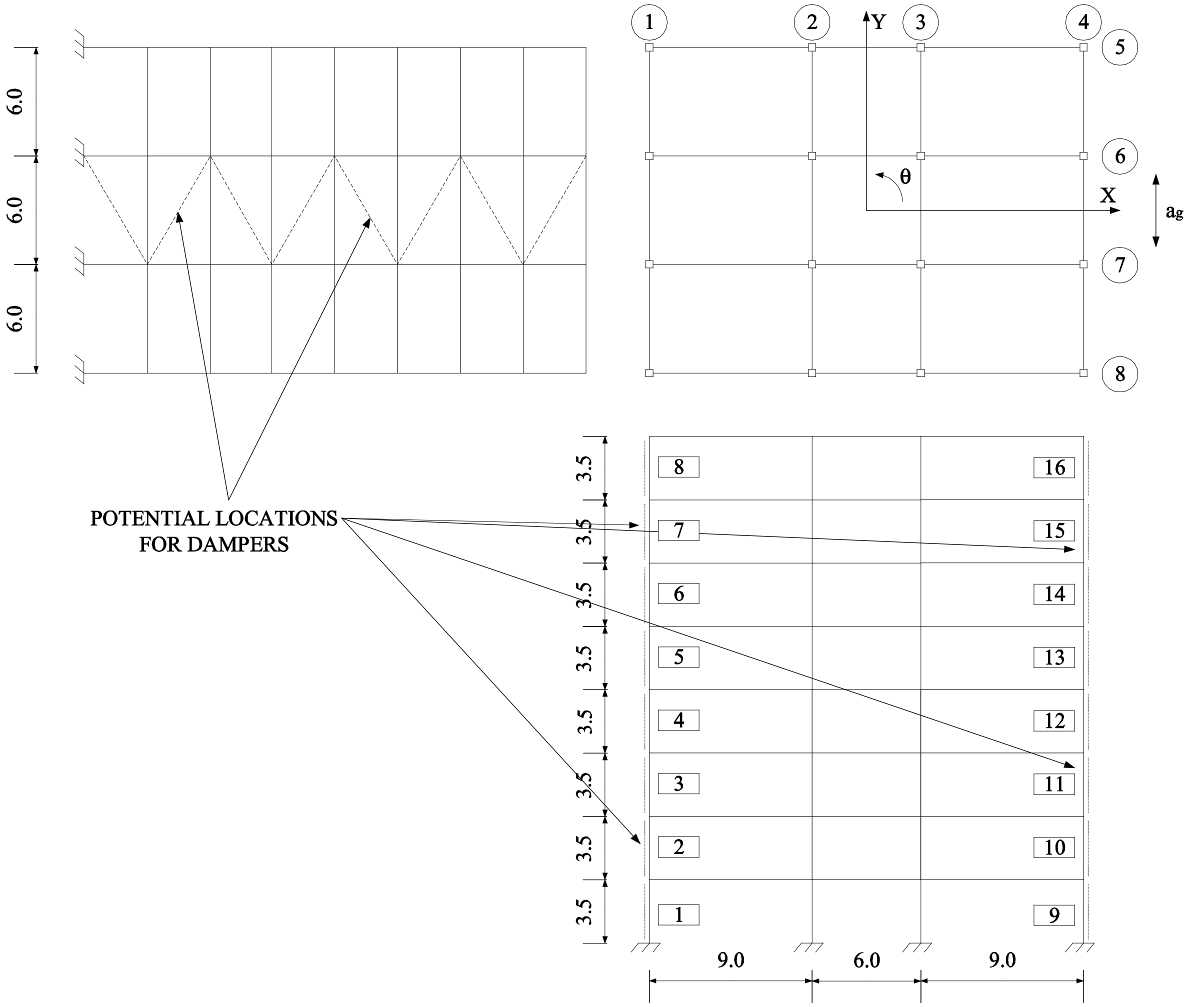

Fig. 5 - Asymmetric frame structure for the numerical example

The optimization problem was solved with the following parameters: C_l=100; C_m=1 1/kN$^{0.5}$; C_p=50; population size = 350; maximum number of iterations = 800; to avoid solutions influenced by local minima 10 different analyses were performed choosing the best solution among them. The variables y_1 and y_2 were bounded as follows: $0 \leq y_1 \leq 0.5$ and $0.5 \leq y_2 \leq 1$. Regarding the dampers, the exponent α considered was 0.35 and the coefficient ρ was for this example equal to 1.0765.

Out of the 10 analyses, the analysis which led to the best solution converged after 194 generations obtaining the values y_1=0.3183 and y_2=0.50003, corresponding to the damper sizes c_1=636.61 kN(s/mm)$^\alpha$ with associated stiffness k_{eq1}=685.27 kN/mm), and c_2=1000.06 kN(s/mm)$^\alpha$ with associated stiffness k_{eq2}=1076.51 kN/mm. The final value of the objective function was J= 1471.44. Looking at the results, the value of y_2 is very close to the lower bound. It seems that the algorithm tried to reduce the value of y_2 below its lower bound. We thus ran another set of 10 analyses, this time modifying the bounds of y_1 and y_2 as follows: : $0 \leq y_1 \leq 0.45$ and $0.45 \leq y_2 \leq 1$. The analysis which led to the best solution converged after 182 generations obtaining the values y_1= 0.3231 and y_2= 0.4977, corresponding to the damper sizes c_1=646.25 kN(s/mm)$^\alpha$ with associated stiffness k_{eq1}=695.66 kN/mm, and c_2=995.34 kN(s/mm)$^\alpha$ with associated stiffness k_{eq2}=1071.44 kN/mm. The final value of the objective function was J= 1471.35. The chosen locations of the dampers are presented in Fig. 6. The stiffness distribution is equivalent to that of the damping scaled by the coefficient ρ. Fig. 7 presents the inter-story drifts of the structure with the added damping normalized by the allowable value.

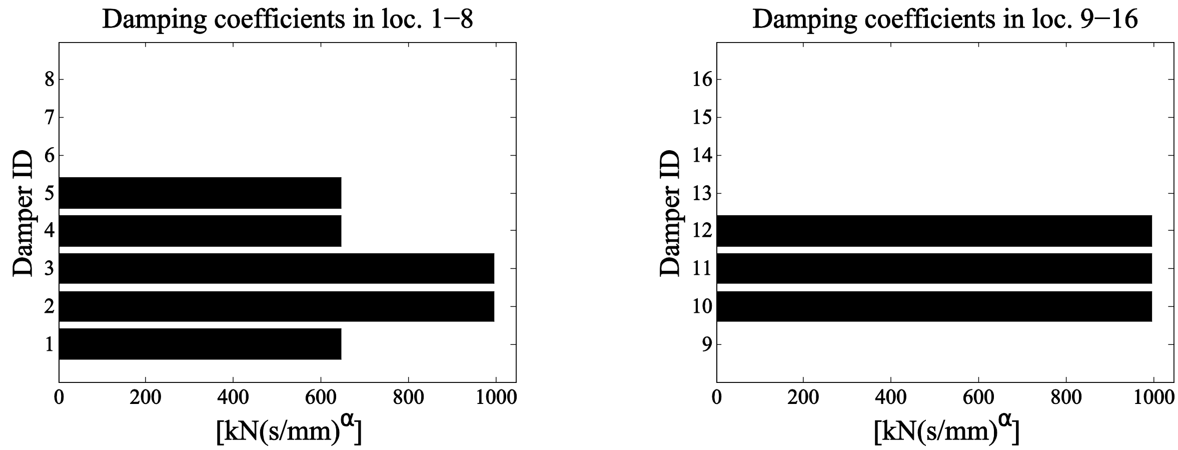

Fig. 6 - Optimal damping distribution. The stiffness distribution is equivalent to the damping distribution, but scaled by the parameter ρ

We can observe that the algorithm chose to allocate eight dampers in the frame, selecting three dampers of the first size-group and five dampers of the second size-group. The same size-group association applies to the coefficients of the equivalent stiffness. For this retrofitting design solution, the inter-story drifts reach the maximum allowable value in location 10. This solution was checked also with the other records from the ensemble. In all cases the peak inter-story drifts were below the allowable one.

To further explore the capabilities of the cost function, we performed another analysis this time changing the value of C_p from 50 to 500. The variables y1 and y2 were bounded as follows: $0 \leq y_1 \leq 0.5$ and $0.5 \leq y_2 \leq 1$. All other parameters were not changed. As expected, the genetic algorithm converged to an optimal solution which involved only one size-group of dampers. The locations occupied by dampers were the same as in Fig. 6, but with all damping coefficients equal to c_2=1096.11 kN(s/mm)^α, (k_{eq2}=1179.91 kN/mm). In particular, out of 10 analyses, the best solution was achieved after 173 iterations, with y_1= 0.3752 and y_2= 0.5480 and a final cost J= 1945.39.

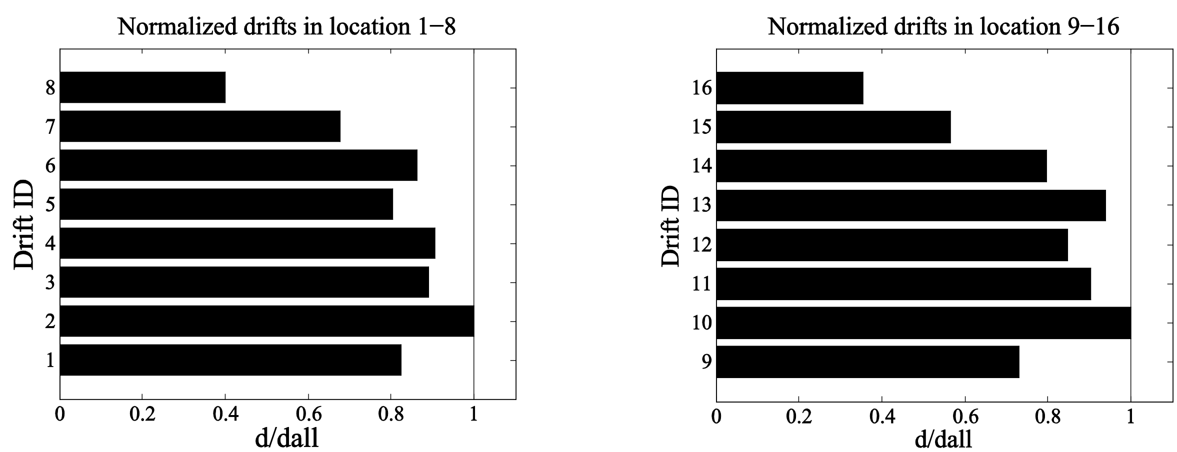

Fig. 7 - Drift distribution corresponding to the optimal damping distribution

The chosen locations of the dampers are presented in Fig. 8, and also in this case the stiffness distribution is equivalent to that of the damping scaled by the coefficient ρ. Fig. 9 presents the inter-story drifts of the structure with the added damping normalized by the allowable value.

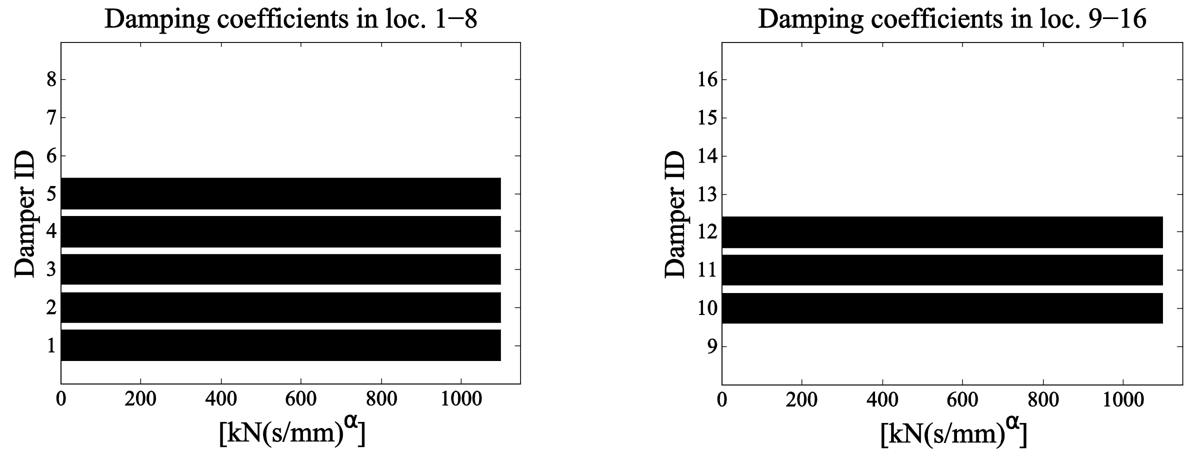

Fig. 8 - Optimal damping distribution for C_p=500. The stiffness distribution is equivalent to the damping distribution, but scaled by the parameter ρ

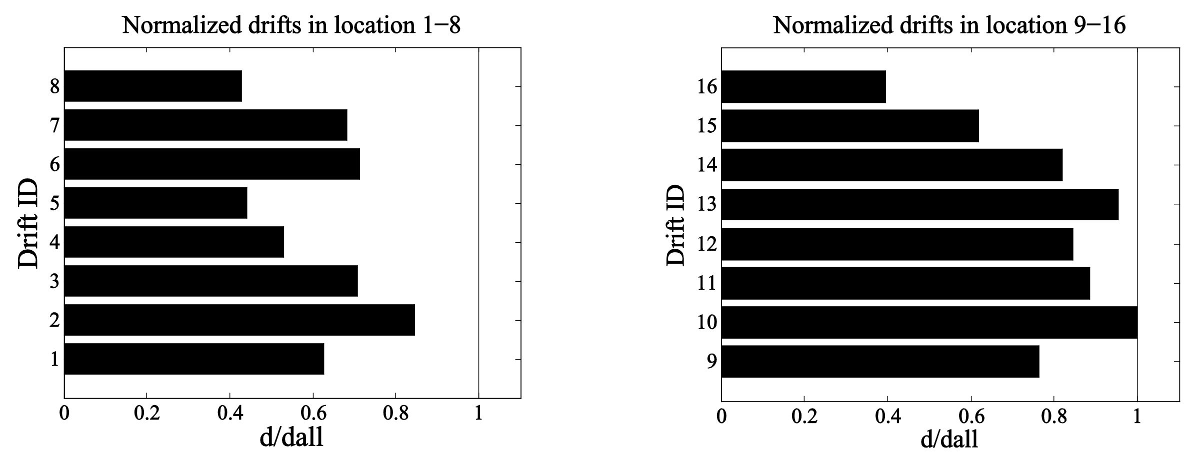

Fig. 9 - Drift distribution for C_p=500 corresponding to the optimal damping distribution

As we already mentioned, the algorithm chose to allocate eight dampers in the frame, all of them belonging to the second size-group. The same size-group association applies to the coefficients of the equivalent stiffness. For this retrofitting design solution, the inter-story drifts reach the maximum allowable value in location 10. This solution was checked also with the other records from the ensemble. In all cases the peak inter-story drifts were below the allowable one.

5. Conclusions

In this paper we presented a novel, effective formulation for the minimum-cost design of nonlinear fluid viscous dampers and their supporting members for seismic retrofitting. The objective function of the optimization problem is the retrofitting cost function, and it is made of three components: The cost associated with the installation of a damper in a specific location in the frame; The manufacturing cost of the dampers; The cost of prototype design and testing. The dampers are modelled with a nonlinear force-velocity behavior defined by a fractional power law. Their interaction with the supporting members and the structure is accounted based on the Maxwell's model for viscoelasticity. The inter-story drifts are evaluated with nonlinear time-history analyses for an ensemble of realistic ground motions, and constrained to an allowable value.

Main contributions of the present work are the realistic cost function and the optimization-based design formulation that involves both the nonlinear fluid viscous dampers and their supporting members. As a result, we can provide practitioners with an effective performance-based design tool for the seismic retrofitting of generic 3-D structures subject to realistic ground motions. The results presented herein show the effectiveness of the presented approach in realistic design problems. In particular, in the example the algorithm identified minimum cost design solutions given the structural performance limitations. Moreover, the work presented in this paper, including the nonlinear damper-brace model, the problem formulation and the results attained, provide an important foundation for further developments on the subject. These will focus on increasing the computational efficiency by reformulating the problem with continuous variables.

6. References

[1] V. V. Bertero, "Performance-based seismic engineering: A critical review of proposed guidelines," *Seismic design methodologies for the next generation of codes (1997),* pp. 1-31, 1997.

[2] M. J. N. Priestley, "Performance based seismic design," in *12th World Conf. on Earthquake Engineering*, Auckland, New Zealand, 2000.

[3] D. Taylor and P. Duflot, "Fluid viscous dampers used for seismic energy dissipation in structures," in *European Conference on Earthquake Engineering*, London, 2002.

[4] O. Lavan and G. F. Dargush, "Multi-objective evolutionary seismic design with passive energy dissipation systems," *Journal of Earthquake Engineering,* vol. 13, pp. 758-790, 2009.

[5] G. D. Hahn and K. R. Sathiavageeswaran, "Effects of added-damper distribution on the seismic response of buildings," *Computers & Structures,* vol. 43, no. 5, pp. 941-950, 1992.

[6] R. H. Zhang and T. T. Soong, "Seismic design of viscoelastic dampers for structural applications," *Journal of Structural Engineering,* vol. 118, no. 5, pp. 1375-1392, 1992.

[7] A. K. Agrawal and J. N. Yang, "Optimal placement of passive dampers on seismic and wind-excited buildings using combinatorial optimization," *Journal of Composite Materials,* vol. 33, pp. 928-940, 1999.

[8] D. L. García, "A simple method for the design of optimal damper configurations in MDOF structures," *Earthquake Spectra,* vol. 17, pp. 387-398, 2001.

[9] G. F. Dargush and R. S. Sant, "Evolutionary aseismic design and retrofit of structures with passive energy dissipation," *Earthquake Engineering and Structural Dynamics,* vol. 34, pp. 1601-1626, 2005.

[10] O. Lavan, "Optimal Design of Viscous Dampers and Their Supporting Members for the Seismic Retrofitting of 3D Irregular Frame Structures," *Journal of Structural Engineering,* vol. 141, no. 11, p. 04015026, 2015.

[11] I. Gidaris and A. Taflanidis, "Performance assessment and optimization of fluid viscous dampers through life-cycle cost criteria and comparison to alternative design approaches," *Bulletin of Earthquake Engineering,* vol. 13, no. 4, pp. 1003-1028, 2015.

[12] Y. Kanno, "Damper placement optimization in a shear building model with discrete design variables: a mixed-integer second-order cone programming approach," *Earthquake Engineering & Structural Dynamics,* vol. 42, no. 11, pp. 1657-1676, 2013.

[13] N. Pollini, O. Lavan and O. Amir, "Towards realistic minimum-cost seismic retrofitting of 3D irregular frames using viscous dampers of a limited number of size groups," in *Second European Conference on Earthquake Engineering and Seismology - 2ECEES,* Istanbul (Turkey), 2014.

[14] O. Lavan and O. Amir, "Simultaneous topology and sizing optimization of viscous dampers in seismic retrofitting of 3D irregular frame structures," *Earthquake Engineering & Structural Dynamics,* vol. 43, no. 9, pp. 1325-1342, 2014.

[15] N. Pollini, O. Lavan and O. Amir, "Towards realistic minimum-cost optimization of viscous dampers for seismic retrofitting," *Bulletin of Earthquake Engineering,* vol. 14, no. 3, pp. 1-28, 2016.

[16] Y. Chen and Y. H. Chai, "Effects of brace stiffness on performance of structures with supplemental Maxwell model-based brace-damper systems," *Earthquake Engineering & Structural Dynamics,* vol. 40, no. 1, pp. 75-92, 2011.

[17] K. Fujita, A. Moustafa and I. Takewaki, "Optimal placement of viscoelastic dampers and supporting members under variable critical excitations," *Earthquake and Structures,* vol. 1, no. 1, pp. 43-67, 2010.

[18] S. Matsuda, "Optimum Design of Maxwell-type Damper System Based on Stochastically Equivalent Damping Factor," in *15th World Conference on Earthquake Engineering (15WCEE),* Lisbon, 2012.

[19] E. Viola and F. Guidi, "Influence of the supporting braces on the dynamic control of buildings with added viscous dampers," *Structural Control and Health Monitoring,* vol. 16, no. 3, pp. 267-286, 2009.

[20] K. Oohara and K. Kasai, "Time-history analysis model for nonlinear viscous dampers," in *Structural Engineers World Congress (SEWC)*, Yokohama, Japan, 2002.

[21] S. Akçelyan and D. G. Lignos, "Dynamic Analyses of 1-Story Moment Frame with Viscous Dampers," [Online]. Available: http://opensees.berkeley.edu/wiki/index.php/Dynamic_Analyses_of_1-Story_Moment_Frame_with_Viscous_Dampers.

[22] TaylorDevices, *Personal communication,* 2015.

[23] A. Seleemah and M. C. Constantinou, "Investigation of seismic response of buildings with linear and nonlinear fluid viscous dampers," 1997.

[24] A. Quarteroni, R. Sacco and F. Saleri, Numerical mathematics (Vol. 37), Springer Science & Business Media, 2010.

[25] W. K. Tso and S. Yao, "Seismic load distribution in buildings with eccentric setback," *Canadian Journal of Civil Engineering,* vol. 21, no. 1, pp. 50-62, 1994.

[26] O. Lavan and R. Levy, " Optimal peripheral drift control of 3D irregular framed structures using supplemental viscous dampers," *Journal of Earthquake Engineering,* vol. 10, no. 06, pp. 903-923, 2006.